Desalination and Water Treatment
www.deswater.com
doi: 10.1080/19443994.2014.966761

57 (2016) 366–381
January

Taylor & Francis
Taylor & Francis Group

Sorption behavior and mechanism investigation of formic acid removal by sorption using an anion-exchange resin

Xiaoqing Lin[a,b], Lian Xiong[a,b], Chao Huang[a,b], Xiaoyan Yang[b,c], Haijun Guo[a,b], Xuefang Chen[b,c], Xinde Chen[a,b,*]

[a]*Guangzhou Institute of Energy Conversion, Chinese Academy of Sciences, Guangzhou 510640, P.R. China, Tel. +86 20 87020234; emails: linxq@ms.giec.ac.cn (X. Lin), xionglian@ms.giec.ac.cn (L. Xiong), huangchao@ms.giec.ac.cn (C. Huang), guohj@ms.giec.ac.cn (H. Guo), Tel. +86 20 37213916; email: cxd_cxd@hotmail.com (X. Chen)*
[b]*Key Laboratory of Renewable Energy, Chinese Academy of Sciences, Guangzhou 510640, P.R. China, Tel. +86 20 87020234; emails: xiaoyanzi0407@163.com (X. Yang), chenxf@ms.giec.ac.cn (X. Chen)*
[c]*Graduate University of Chinese Academy of Sciences, Beijing 10049, P.R. China*

Received 14 March 2014; Accepted 13 September 2014

ABSTRACT

In this work, D-II07 resin was used to remove formic acid from aqueous solution. A series of operational conditions including solution pH, adsorbent dose, temperature and initial formic acid concentration on formic acid uptake was evaluated. D-II07 resin showed a good uptake at neutral pH. Removal of formic acid was rapid and equilibrium was reached within 2 h of contact. The results demonstrated that the sorption equilibrium data were well fitted by bi-Langmuir isotherm model and the maximum sorption capacity was negatively affected with increasing temperature. Thermodynamic studies performed indicated that the sorption process was spontaneous and exothermic in nature. Furthermore, the sorption kinetic of formic acid was simulated successfully by the macropore diffusion model. The effective pore diffusivity (D_p) was dependent on temperature, but independent of initial formic acid concentration, and was 1.846×10^{-10}, 3.652×10^{-10}, and 5.552×10^{-10} $m^2\ s^{-1}$ at 298, 318, and 338 K, respectively. In summary, D-II07 resin is a promising valuable adsorbent to remove formic acid from the diluted wastewater streams or fermentation broth.

Keywords: Formic acid; Mechanism investigation; Resin; Sorption

1. Introduction

It is well known that formic acid (or methanoic acid) is an important raw material in chemical industries, which is used as an intermediate in the production of food preservatives and pharmaceuticals such as enzymes, antibacterial agents, caffeine, artificial sweeteners, plant protection agents, dyes, flavors, and perfume ingredients [1,2]. In recent years, the use of biotechnological method for producing monocarboxylic acids has attracted a considerable attention due to its potential advantages in both economical and environmental aspects [2]. Many fermentation processes produce dilute solutions of carboxylic acids which are either products or by-products of the process [3,4]. In addition, wastewaters of industrial (pharmaceutical, polymer, food, leather, textile, etc.) effluents containing low concentration of monocarboxylic acids are

*Corresponding author.

often encountered [1]. If the concentrations of these monocarboxylic acids exceed certain threshold levels, they will be toxic to micro-organisms and will inhibit cell growth [5]. Advanced treatment of wastewater streams to meet future water quality standards and circular utilization has been acknowledged as a noteworthy expenditure to the industry and environment [1].

Because of the above-mentioned reasons, the separation of these carboxylic acids is of interest in terms of both environmental and economic effects. However, the removal of carboxylic acids from wastewater streams, fermentation broth, or aqueous solutions presents a major challenge due to the complex nature of fermentation broth and high affinity for water [6,7]. By now, several acid recovery techniques, including precipitation [8], solvent extraction [1], electrodialysis [9], adsorption [7], ion-exchange [10–16], have been investigated and employed to selectively remove the carboxylic acids from wastewater or fermentation broth. Among these techniques, adsorption and ion-exchange are undoubtedly advanced processes for separating the acids from aqueous or wastewater streams and they can be coupled with fermentation process due to its low cost for industrialization.

Weakly basic ion exchangers are frequently used for the recovery of carboxylic acid from aqueous solution, wastewater, or fermentation broth [7,10,11]. However, the detailed adsorption equilibrium and kinetics of formic acid were sparsely reported in the literature so far [7], and many valuable empirical equations for sorption have been built. Moreover, little work has been focused on the model building for predicting the sorption behavior of different systems. In other words, most of the results of the above studies could be applied merely in some special situations. For future industrial application, it is critical to have systematically statistical theory on the formic acid sorption. Therefore, in this work, a tailor-made ionic exchanger D-II07 resin was used to adsorb formic acid from its aqueous solution. The formic acid concentration was investigated in the range of 0–10 g L^{-1}. The sorption properties of formic acid onto D-II07 resin were investigated systematically. The effects of initial solution pH and adsorbent dose on the sorption capacity of formic acid were firstly performed. Subsequently, the sorption isotherms of formic acid at different temperatures were determined under the selected pH condition. Some thermodynamic sorption parameters such as the Gibbs free energy change (ΔG°), the enthalpy change (ΔH°), and the entropy change (ΔS°) were estimated by correlation [17]. Afterward, the effects of initial formic acid concentration and temperature on the rate of sorption were investigated. The macropore diffusion model, pseudo-first-order, and pseudo-second-order models were used to predict the formic acid concentration decay curves. The sorption equilibrium data and the model parameters reported in this study will be of great value in designing a chromatographic process for recovering formic acid from wastewater streams and fermentation broth.

2. Material and methods

2.1. Material

D-II07 anion-exchange resin, with a tertiary amine functional group, was kindly supplied by the Guangzhou Institute of Energy Conversion, Chinese Academy of Sciences (Guangzhou, China). The D-II07 anion-exchange resin used in this study was in OH^{-} form. The physical properties of the resin are listed in Table 1. Before use, the resin was firstly soaked in 95% ethanol solution for 24 h and then in 1 M hydrochloric acid and 1 M sodium hydroxide for 8 h to remove monomers, preservative agents, and polymerization residuals which are trapped inside the pores during synthesis [18]. Finally, the resin was rinsed at neutral pH with deionized water. Formic acid used in this study was of analytical reagent grade, which was purchased from the Sinopharm Chemical Reagent Co., Ltd and used without further purification.

2.2. Methods

2.2.1. Characterization of D-II07 resin

The morphology and surface texture of D-II07 resin was identified by a high resolution field emission scanning electron microscope (FE-SEM, Hitachi S-4800, Japan) operated at 1 kV and 10 μA. The Brunauer–Emmett–Teller (BET) surface area, total pore volume, and average pore diameter of D-II07 resin were detected by nitrogen adsorption–desorption isotherms at −196°C using an ASIQMO002-2 analyzer (Quantachrome, US). Prior to measurement, the resin was degassed under vacuum at 90°C for 16 h for the removal of water and impurities [19]. The pore distribution of the resin was calculated using the Barrett–Joyner–Halenda method to the nitrogen desorption data.

2.2.2. Effect of initial solution pH on formic acid uptake

Experiments to determine the effect of solution pH on the sorption of formic acid onto D-II07 resin were conducted by equilibrating the sorption mixture with the resin and formic acid aqueous solution at different pH values between 1 and 10. The pH of formic acid

Table 1
Characteristic properties of D-II07 weakly base ion-exchange resin

Resin	D-II07
Matrix structure	Macroporous polystyrene divinylbenzene
Functional groups	$-N(CH_3)_2$
Physical form	Insoluble, milkiness beads
Ionic form	OH^-
Porosity (%)	32.5
Surface area ($m^2\ g^{-1}$)	36.071
Pore volume ($cm^3\ g^{-1}$)	0.478
Average pore diameter (nm)	53
Total exchange capacity (mmol g^{-1})	≥4.8
Water retention capacity (%)	48–58
Skeletal density (g mL^{-1})	0.65–0.72
Wet density (g mL^{-1})	1.05
Uniformity coefficient	<1.60
Particle size range (mm)	0.8
Operating pH range	0–9
Thermal stability (K)	273–343

solution was adjusted by adding dilute hydrochloric acid and sodium hydroxide. Batch sorption experiments were performed using 100 mL Erlenmeyer flasks containing 1 g of D-II07 resin and 50 mL of 5 g L^{-1} formic acid solution. The flasks were placed in a thermostatic shaker at 160 rpm and 298 K for 140 min. It is observed from the preliminary kinetic sorption experiment that the sorption can reach equilibrium within 140 min. At the end of the sorption, the liquid phase was sampled with a syringe equipped with a filter (Spartan 30/0.45 RC [0.45 μm]) to remove suspended solids. The concentration of the formic acid was analyzed by high performance liquid chromatography (HPLC). The amount of formic acid adsorbed onto D-II07 resin at equilibrium q_e (mg g^{-1}) was calculated with Eq. (1) [18].

$$q_e = \frac{(C_0 - C_e) \cdot V}{m} \quad (1)$$

where C_0 and C_e are the concentrations of formic acid in the aqueous phase at initial and equilibrium conditions (g L^{-1}), respectively. V is the volume of aqueous solution (L); m is the mass of the wet resin (g).

2.2.3. Effect of adsorbent dose on the removal extent of formic acid

Different adsorbent doses (1, 2, 3, 4, and 5 g) of D-II07 resin were added into 50 mL formic acid solutions in which the concentration of formic acid was 5 g L^{-1} and the initial solution pH was kept original without any adjustment. The sorption procedures were the same as described for the effect of pH on formic acid uptake.

2.2.4. Equilibrium experiments

The equilibrium sorption experiments of formic acid adsorbed onto D-II07 resin were carried out at three temperatures of 298, 318, and 338 K, respectively. Sorption equilibrium data were determined by contacting about 1 g of resin with 50 mL of formic acid aqueous solution at a series of different concentrations from 0 to 10 g L^{-1}, which corresponded to the concentration range of an actual lipid fermentation broth of *T. fermentans* [4]. The sorption procedures were the same as described for the effect of pH on formic acid uptake.

2.2.5. Batch sorption kinetic studies

The kinetic experiments were performed to evaluate the influence of contact time, at different initial concentrations of formic acid (1, 5, and 10 g L^{-1}) at various temperatures (298, 318, and 338 K), on sorption. In the kinetic experiments, about 20 g of the resin and 1,000 mL of formic acid solution were quickly introduced into a cone-shaped flask. Then, the flask was shaken in a thermostat water bath with agitation at 160 rpm. one millilitre of the solution was sampled at different time intervals with a syringe, filtered immediately, and analyzed later by HPLC. The concentration of the residual solution was determined

until the sorption equilibrium was reached, and the amount of formic acid on resin at any contact time, t, was calculated as:

$$q_t = \frac{C_0 V_0 - C_t(V_0 - \sum_{i=1}^{n} V_i)}{m} \quad (2)$$

where C_0 and C_t are the concentrations of formic acid in the aqueous phase at initial and contact time t (g L^{-1}), respectively, q_t is the sorption capacity of formic acid at contact time t (mg g^{-1}), m is the mass of the wet resin (g), and i is the number of sampling times. V_0 and V_i are the initial volumes of the aqueous solution (L) and the sampling volume (L), respectively.

2.2.6. Analytical methods

Determination of the concentration of formic acid in the aqueous solution was performed by HPLC (Waters 2685 systems, Waters Corp., USA) equipped with an ultraviolet detector (Waters 2489). Separation was achieved on an Amines HPX-87H anion-exchange column (300 mm × 7.8 mm, Bio-Rad Corp., USA) using 5 mM sulfuric acid as mobile phase at a flow rate of 0.6 mL min^{-1} and the column temperature was maintained at 65°C. The detector wavelength was set at 210 nm. External standards were prepared for calibration.

All the sorption experiments in this research were carried out at least three times to ensure reproducibility and it was found that the errors for all tests were less than 10%. Therefore, the average values of the three data-sets were used as sorption data.

3. Results and discussion

3.1. Characterization of the anion-exchange resin D-II07

The morphology and surface texture of D-II07 resin observed by FE-SEM is presented in Fig. 1(A). As it depicted, D-II07 resin had a spherical form and a rough internal surface. Fig. 1(B) shows the N_2 adsorption–desorption isotherms. The values of BET surface area, total pore volume, and average pore diameter of D-II07 resin are listed in Table 1. As shown in Fig. 1(B), the N_2 adsorption–desorption isotherms coincided completely with a relative pressure (P/P_0) below 0.9, indicating that the micropores and mesopores did not exist in D-II07 resin. However, the visible hysteresis loop of desorption isotherm with a relative pressure (P/P_0) over 0.9 indicated that D-II07 resin had a structure containing macropores. These analyses agreed with the pore diameter distribution in Fig. 1(C). In addition, it can be observed from Fig. 1(C) that the macropores are the main pores for D-II07 resin and the average pore diameter is 53 nm.

3.2. Effect of the initial solution pH on the sorption

Formic acid is a weak acid, which could undergo dissociation depending on the solution pH (Eq. (3)). The distribution of various formic acid species vs. pH is presented in Fig. 2(A). The formic acid dissociation constant pKa is equal to 3.75 at a temperature of 298 K [20,21]. It can be observed from Fig. 2(A) that the formic acid exists mostly in its non-ionized form in the lower pH range, e.g. pH < 1, while it exists mostly in its ionized form in the higher pH range, e.g. pH > 6. Theoretically, only negatively charged formate ions can be exchanged with hydroxyl ions in the D-II07 resin according to the reactions shown in Eq. (4). Hence, the formic acid uptake onto the anionic exchanger would depend on the solutions pH.

$$HCOOH \rightleftharpoons HCOO^- + H^+ \quad (3)$$

$$R^+ - OH^- + HCOO^- \rightleftharpoons R^+ - HCOO^- + OH^- \quad (4)$$

Fig. 2(B) shows the effect of the initial solution pH (1–10) on the sorption process of formic acid by D-II07, a weakly basic anion-exchange resin. As the initial solution pH changed from 1 to 3, the sorption capacity of formic acid onto D-II07 resin was found to increase drastically at first with an increase in the initial solution pH, and then declined sharply as the initial solution pH increased from pH 3 to 6. After that, the sorption capacity of formic acid onto D-II07 resin remained basically unchangeable of 11 mg g^{-1} as the initial solution pH increased from pH 6 to 10. The formic acid did not retain onto the D-II07 resin at the solution pH of 1. This was due to the fact that more than 99.8% of formic acid exists in its molecular form at the initial solution pH of 1 (Fig. 2(A)), which could not exchange with hydroxyl ions in the D-II07 resin and, thus, could not be adsorbed. However, this result could give us a hint for the preliminary selection of desorbent in the following desorption process. The value of maximum sorption capacity of formic acid (q_e = 103 mg g^{-1}) onto D-II07 resin was achieved at pH 2.34, in which the solution pH was kept original without any adjustments and the initial formic acid concentration was 5 g L^{-1}. The quick reduction in the capacity of formic acid adsorbed in the pH range from 3 to 10 probably attributed to the effect of competitive

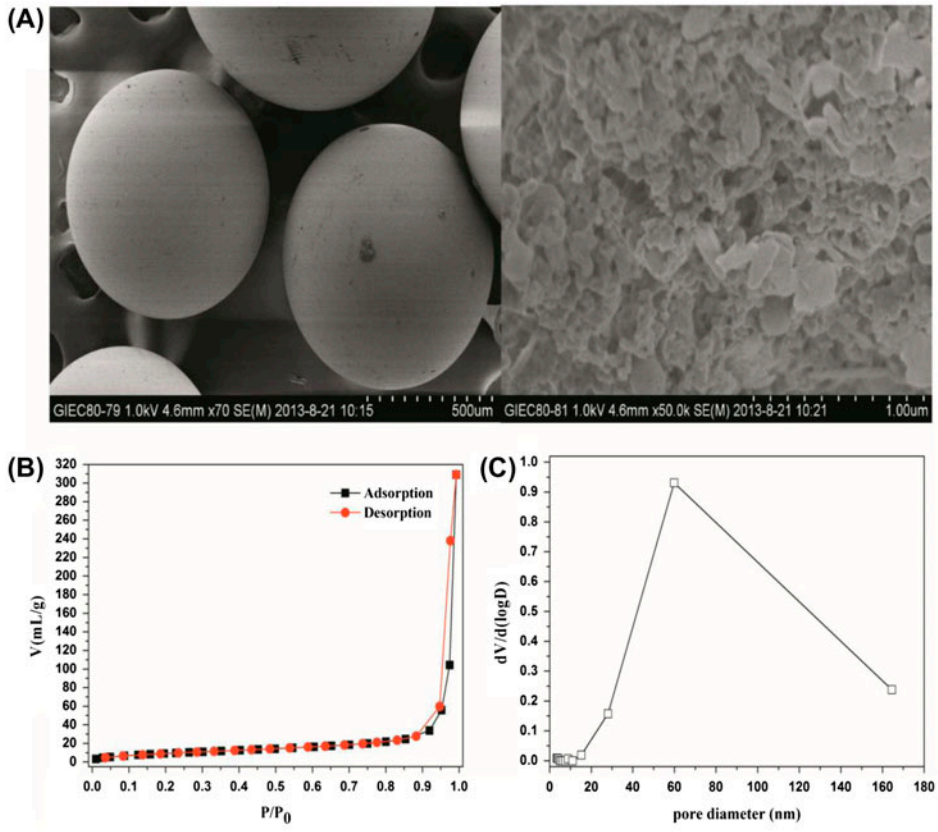

Fig. 1. Characterization of D-II07 resin: (A) SEM image of D-II07 resin; (B) N_2 adsorption–desorption isotherms; and (C) pore diameter distribution.

binding between hydroxyl ions and formate ions for the adsorption sites that are present on the surface of the resin [22,23]. At higher initial solution pH, an excess of hydroxyl ions competed effectively with formate ions for adsorption sites, resulting in a lower level of formic acid uptake.

In order to explain the phenomenon, the solution pH values before and after the sorption were determined and also represented in Fig. 2(B). Interestingly, the solution pH after the sorption was higher than its original in the pH range from 1 to 8. This phenomenon indicated that the formate ions were adsorbed and exchanged with hydroxyl ions, resulting in the transfer of hydroxyl ions from the resin phase into the solution phase. These hydroxyl ions could induce formic acid dissociation (according to Eq. (3)). Consequently, more formate ions were available to be adsorbed. This is in the case of pH which is equal to 2.34 formic acid solutions. However, the exchange process is reversible. In other words, plenty of hydroxyl ions existing in the solution can move the process toward the opposite direction. This is the reason why the sorption capacity was reduced with further increase in the initial solution pH. The exchanged hydroxyl ions were located at pH ranging from 3 to 8, resulting in the significant increase in solutions pH. It could be concluded that the optimum pH of the sorption of formic acid onto D-II07 resin should be the neutral pH. Therefore, all the following sorption experiments were conducted without adjusting the pH of formic acid solutions. While in the range of pH > 8, the pH at equilibrium shows a lower value than the initial pH of solution. This phenomenon was similar to previous reports on hexavalent chromium ions adsorption onto modified sand [24]. At higher pH, $HCOO^-$ was present in aqueous solutions. In this condition, the presence of large number of OH^- hinders the diffusion of formate ions. As the solution pH increases, not only less functional groups are deprotonated but also more number of OH^- compete with the formate ions for the active surface sites.

3.3. Effect of adsorbent dose on the extent of removal of formic acid

The effect of adsorbent dose on the extent of removal of formic acid at neutral pH is shown in Fig. 3(A). It was apparent from Fig. 3(A) that the

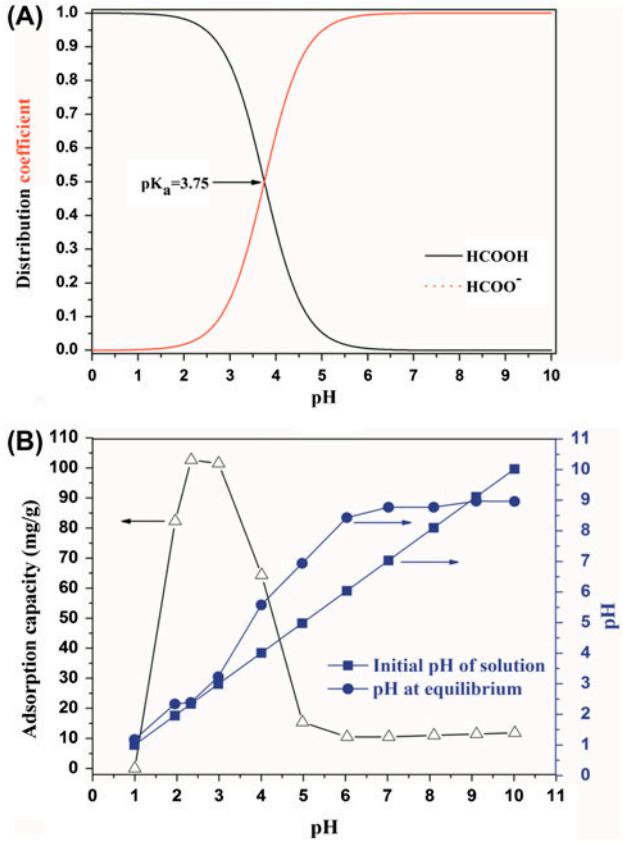

Fig. 2. (A) The distribution coefficients of two forms of formic acid in aqueous solutions at variable pHs and (B) the effect of solution pH on the sorption capacity of formic acid onto D-II07 resin at 298 K (C_0 = 5 g L^{-1}).

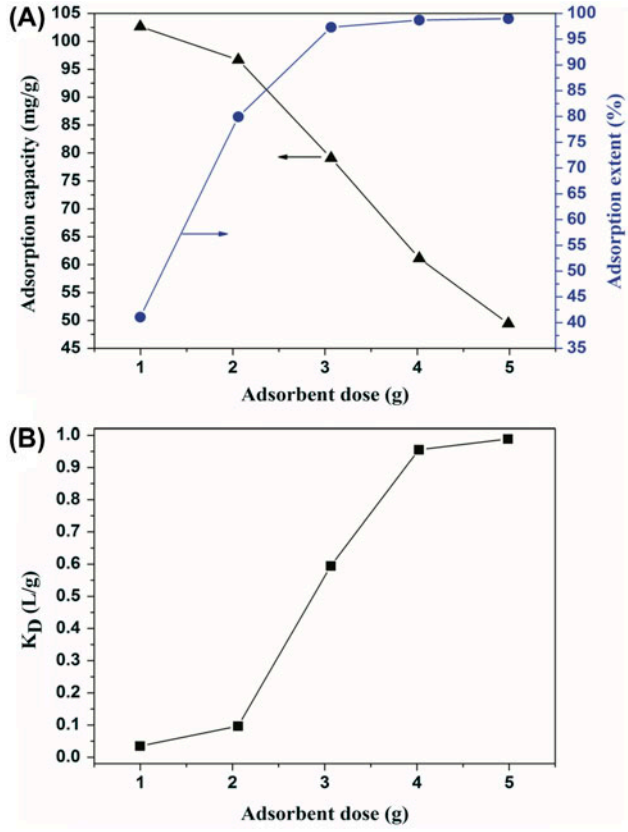

Fig. 3. (A) Effect of adsorbent dose on removal extent and adsorption capacity of formic acid and (B) plot of K_D values as a function of adsorbent dose.

extent of formic acid sorption efficiency increased by increasing the resin amount. The extent of formic acid removal was 41.1% for 1 g of resin, while it was increased dramatically to 97.3% for 3 g of resin. However, it was worth noting that there was only a tiny change in the extent of formic acid sorption when the resin dose was over 3 g. For example, the removal extent was 99% for 5 g of resin. This phenomenon was probably due to the fact that the number of available adsorption sites increases with an increase in the resin dose, resulting in an increase in removal efficiency [25]. Furthermore, it was observed that the higher resin dose would result in lower sorption capacity of formic acid onto D-II07 resin at a fixed formic acid concentration of 5 g L^{-1}. The decrease in the sorption capacity can be attributed to the fact that some of the adsorption sites remain unsaturated during the sorption process. This is consistent with the statement that the adsorption sites of the resin are heterogeneous [23,26]. According to the surface site heterogeneous model, the surface of resin is composed of sites with a spectrum of binding energies [23]. At low resin dose, all types of surface sites are entirely exposed and the sorption on the surface is saturated faster, resulting in a higher sorption capacity. However, at higher resin amount, the availability of higher energy sites decreases with a larger fraction of lower energy sites occupied, showing a lower sorption capacity.

The distribution coefficient K_D can be employed to describe the binding ability of adsorbent surface for an element, which is determined from the following equation [27]:

$$K_D = \frac{C_S}{C_W} \tag{5}$$

where C_S (g g^{-1}) and C_W (g L^{-1}) are the concentrations of formic acid in resin particles and solution, respectively. It can be seen from Fig. 3(B) that the distribution coefficient K_D increased with an increase in resin dose, which indicated that the surface of D-II07 resin should be heterogeneous. The relationship between distribution coefficient K_D and surface site was

expressed as [26]: "if the surface is homogeneous, the distribution coefficient K_D at a given pH should not change with adsorbent dose."

3.4. Sorption isotherm

The sorption isotherms express the special relation between the concentration of the adsorbate and its degree of accumulation onto the adsorbent surface when the sorption process reached to an equilibrium state at a constant temperature [18]. Therefore, it is important to establish the most appropriate correlation for the equilibrium curves that can be used to optimize the design of a sorption system. Fig. 4(A)–(C) show the equilibrium sorption isotherm of formic acid (point) onto D-II07 resin at various temperatures. It was clearly observed from Fig. 4(A)–(C) that the sorption capacity of formic acid onto D-II07 resin increased rapidly at low initial concentrations at different temperatures, indicating a high affinity between the adsorbate and adsorbent. However, the adsorbed amounts of formic acid increased slightly at high initial concentrations.

In this study, five commonly used isotherm models, namely Langmuir, Freundlich, Sips, Temkin, and bi-Langmuir, were applied to fit the equilibrium data of sorption of formic acid onto D-II07 resin at different temperatures.

The Langmuir isotherm model [28] is based on the assumption that the monolayer sorption occurs onto a surface containing a finite number of sorption sites of uniform strategies of sorption with no transmigration of adsorbate in the plane of surface, which can be expressed by the following equation:

$$q_e = \frac{q_{max} k_L C_e}{1 + k_L C_e} \tag{6}$$

where q_e is the equilibrium sorption capacity (mg g^{-1}); C_e is the equilibrium formic acid concentration in the liquid phase (g L^{-1}); q_{max} is the maximum saturated sorption capacity (mg g^{-1}); k_L is Langmuir constant (L g^{-1}).

Furthermore, the essential characteristics of Langmuir isotherm can be expressed by a dimensionless separation factor or equilibrium parameter, R_L, defined by Webi and Chakravort [29] as:

$$R_L = \frac{1}{1 + K_L C_0} \tag{7}$$

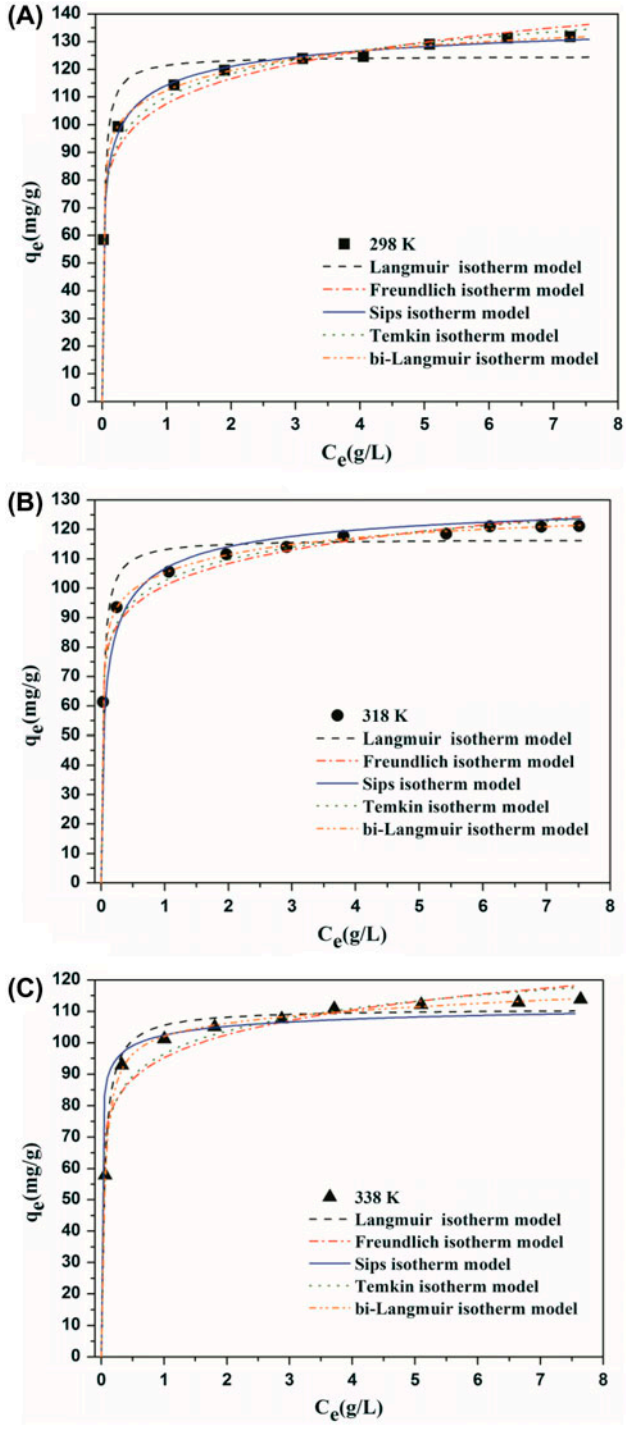

Fig. 4. Sorption equilibrium data (point) fitted by Langmuir (dash), Freundlich (dash-dot), Sips (solid), Temkin (dot), and bi-Langmuir (dash-dot-dot) isotherm models for the sorption of formic acid onto D-II07 resin at different temperatures: (A) T = 298 K; (B) T = 318 K; and (C) T = 338 K.

where k_L is the Langmuir constant (L g^{-1}) and C_0 is the initial formic acid concentration (g L^{-1}). The parameter R_L indicates that the type of isotherm can be unfavorable ($R_L > 1$), linear ($R_L = 1$), favorable ($0 < R_L < 1$), or irreversible ($R_L = 0$).

The Freundlich isotherm model [30] assumes that the sorption energy of the adsorbate binding to the adsorbent depends on the availability of sorption sites, which can be expressed as:

$$q_e = k_F C_e^{1/n_F} \tag{8}$$

where q_e is the equilibrium sorption capacity (mg g^{-1}); C_e is the equilibrium formic acid concentration in the liquid phase (g L^{-1}); k_F (mg g^{-1}(L $g^{-1})^{1/n_F}$) and $1/n_F$ are the Freundlich constants. The parameter $1/n_F$ indicates how favorable the sorption process is; the value of $1/n_F$ below 1 indicates a normal Langmuir isotherm, while $1/n_F$ above 1 is indicative of cooperative sorption [31]. The value of $1/n_F$ ranging between 0 and 1, which is a measure of sorption intensity or surface heterogeneity, and as the value of $1/n_F$ got closer to 0, the sorption became more heterogeneous [31,32].

The Sips isotherm model [33] is a combination of Langmuir and Freundlich isotherm models which can be described as:

$$q_e = \frac{q_{max} k_S C_e^{n_s}}{1 + k_S C_e^{n_s}} \tag{9}$$

where q_e is the equilibrium sorption capacity (mg g^{-1}); C_e is the equilibrium formic acid concentration in the liquid phase (g L^{-1}); q_{max} is the maximum saturated sorption capacity (mg g^{-1}); k_S ((L $g^{-1})^{1/n}{}_S$) and n_S are the Sips isotherm model parameters. The Sips isotherm reduces to Langmuir isotherm when the value of n_S is equal to 1.

The Temkin isotherm is based on the heat of sorption of the ions, which is due to the sorbate/sorbent interactions taken in linear form. Temkin isotherm model is given by Choy et al. [34]:

$$q_e = \frac{RT}{b_{Te}} \ln (a_{Te} C_e) \tag{10}$$

where q_e is the equilibrium sorption capacity (mg g^{-1}); C_e is the equilibrium formic acid concentration in the liquid phase (g L^{-1}); b_{Te} is the Temkin constant related to heat of sorption (J mol^{-1}); a_{Te} is the Temkin isotherm constant (L g^{-1}); R is the general gas constant (8.314 J mol^{-1} K^{-1}); T is the absolute temperature (K).

The bi-Langmuir model assumes that the surface contains two different active sites with different affinities toward compounds [35]:

$$q_e = \frac{q_{max\,1} k_{L1} C_e}{1 + k_{L1} C_e} + \frac{q_{max\,2} k_{L2} C_e}{1 + k_{L2} C_e} \tag{11}$$

where q_e is the equilibrium sorption capacity (mg g^{-1}); C_e is the equilibrium formic acid concentration in the liquid phase (g L^{-1}); q_{max1} and q_{max2} are the maximum sorption capacities of two different adsorption sites (mg g^{-1}); and k_{L1} and k_{L2} are sorption energies related to these sorption sites (L g^{-1}).

All the isotherm model parameters were evaluated by non-linear regression using Matlab software. The residual root mean square error (RMSE) and the χ^2 test, together with the correlation coefficient (R^2), were used to evaluate the fitness of the model calculations to the experimental data.

The RMSE can be defined as:

$$\mathrm{RMSE} = \sqrt{\frac{1}{m-2} \sum_{i=1}^{m} (q_{exp} - q_{cal})^2} \tag{12}$$

The χ^2 test can be described as:

$$\chi^2 = \sum_{i=1}^{m} \frac{(q_{exp} - q_{cal})^2}{q_{cal}} \tag{13}$$

where the subscripts "exp" and "cal" are the experimental and calculated values, respectively, and m is the number of samples.

Fig. 4 shows the equilibrium sorption data (points) at three temperatures, together with the prediction curves calculated by the Langmuir (dash lines), Freundlich (dash dot lines), Sips (solid lines), Temkin (dot), and bi-Langmuir (dash-dot-dot) isotherm models, respectively. All the isotherm parameters obtained from the five isotherm models are listed in Table 2. The calculated R_L values at different temperatures were between 0 and 1, representing that the sorption of formic acid onto D-II07 resin was favorable. Moreover, the values of R_L at a constant temperature decreased as the initial concentration increased from 1 to 10 g L^{-1}, which indicated that the sorption process was more favorable at higher initial concentration. It can also be seen from Table 2 that all $1/n_F$ values obtained from the Freundlich isotherm model were below one at all three temperatures, indicating favorable sorption. It can be observed from Fig. 4(A)–(C) and Table 2 that the sorption capacity of formic acid

Table 2
Isotherm parameters of each isotherm model for the sorption of formic acid onto D-II07 resin at different temperatures

Isotherm models		Temperature (K)		
		298	318	338
Langmuir	q_{max} (mg g^{-1})	124.844	116.728	110.876
	K_L (L g^{-1})	35.342	31.337	19.964
	R_L	0.00282–0.0229	0.00318–0.0243	0.0050–0.0396
	R^2	0.898	0.903	0.965
	RMSE	7.465	5.831	3.315
	χ^2	3.599	2.663	0.777
Freundlich	$1/n_F$	0.117	0.104	0.107
	K_F (mg g^{-1}(L $g^{-1})^{1/n_F}$)	107.515	100.842	95.213
	R^2	0.941	0.940	0.872
	RMSE	5.688	3.397	6.336
	χ^2	2.935	2.184	3.797
Sips	q_{max} (mg g^{-1})	146.219	133.615	117.000
	k_S ((L $g^{-1})^{1/n_S}$)	3.570	3.946	7.024
	n_S	0.429	0.567	0.348
	R^2	0.994	0.995	0.992
	RMSE	1.615	1.618	1.411
	χ^2	0.157	0.182	0.144
Temkin	b_{Te} (J mol^{-1})	204.151	253.972	269.686
	a_{Te} (L g^{-1})	8,627.287	18,931.030	10,512.280
	R^2	0.981	0.976	0.931
	RMSE	3.434	3.078	4.962
	χ^2	0.933	0.886	2.094
bi-Langmuir	q_{max1} (mg g^{-1})	39.094	32.152	24.404
	k_{L1} (L g^{-1})	0.449	0.482	0.080
	q_{max2} (mg g^{-1})	101.842	96.425	105.568
	k_{L2} (L g^{-1})	63.261	57.058	18.774
	R^2	0.999	0.999	0.999
	RMSE	0.920	0.349	1.352
	χ^2	0.052	0.024	0.105

onto D-II07 resin decreased with increasing temperature, which suggested that the sorption process was probably exothermic. Comparing these five isotherm models, the bi-Langmuir isotherm model gave the highest correlation coefficients (R^2) and lowest RMSE and χ^2 values at all three temperatures studies, indicating that the sorption of formic acid onto D-II07 resin was best described by bi-Langmuir model. This observation was different from previous reports on formic acid sorption onto Amberlite IRA-67, [7] probably because of the differences in original adsorbent.

3.5. Sorption thermodynamics

Sorption thermodynamics is of great importance for exploring the adsorbents and demonstrating the sorption process [36]. In this paper, the thermodynamic parameters such as the Gibbs free energy change (ΔG°), the enthalpy change (ΔH°), and the entropy change (ΔS°) had been calculated, respectively. The Gibbs free energy change (ΔG°) was calculated using the following equation:

$$\Delta G^\circ = -RT \ln K_0 \quad (14)$$

where R is the universal gas constant (8.314 J mol^{-1} K^{-1}), T is the absolute solution temperature (K), and K_0 is the sorption coefficient, which was calculated from the intercept of ln (C_e/q_e) vs. C_e plot (Fig. 5(A)) [7,37,38].

The results of the calculated K_0 and ΔG° at different temperatures are listed in Table 3. The Gibbs free energy change (ΔG°) during the sorption process at 298, 318, and 338 K were −0.244, −0.186, and −0.093 kJ mol^{-1}, respectively. The negative value of ΔG° indicated the feasibility spontaneous nature of formic acid sorption onto D-II07 resin. It was found that the values of ΔG° decreased with increasing temperature, indicating less driving force and hence resulting

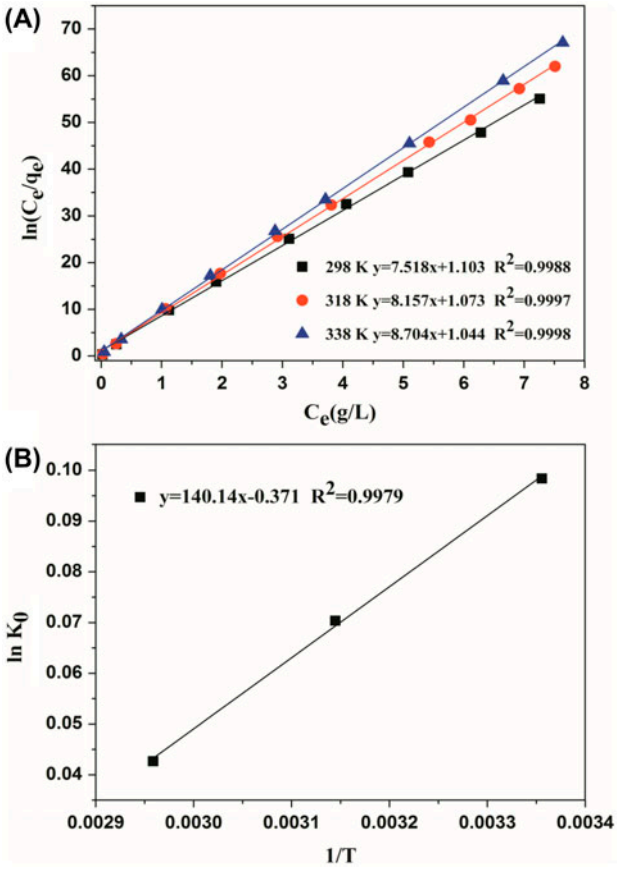

Fig. 5. (A) Plot of ln (C_e/q_e) vs. C_e at different temperatures and (B) plot of ln K_0 against $1/T$.

in less sorption capacity [39]. In addition, the absolute values less than 20 kJ mol^{-1} implied that the sorption was a physical process [37].

According to the Van't Hoff equation [40], the relationship between the sorption coefficient K_0 and temperature is expressed as Eq. (15). The enthalpy change (ΔH°) and the entropy change (ΔS°) were calculated from the slope and intercepts of the plot of lnK_0 vs. $1/T$ (Fig. 5(B)), respectively. The calculated values of ΔH° and ΔS° are listed in Table 3.

$$\ln K_0 = -\frac{\Delta H^\circ}{R}\frac{1}{T} + \frac{\Delta S^\circ}{R} \quad (15)$$

The negative value of ΔH° (Table 3) suggested that the sorption process of formic acid onto D-II07 resin was exothermic in nature. This finding was consistent with the results obtained earlier where the sorption capacity of formic acid onto Amberlite IRA-67 decreased with increasing solution temperature [7]. In addition, the negative value of ΔS° (Table 3) showed that more ordered arrangement of formic acid was shaped on D-II07 surface after sorption [36]. In such case, it will be more profitable in the aspect of process design efficiency, because a lesser number of parameters can be utilized in the design stage.

3.6. Kinetic studies

3.6.1. Effect of solution temperature on formic acid sorption

The effect of solution temperature on the sorption time and sorption rate of formic acid onto D-II07 resin was investigated for a period of 140 min for the initial formic acid concentration of 5 g L^{-1} at 298, 318, and 338 K, respectively. Fig. 6(A) shows the results of contact time experiments carried out at various solution temperatures for formic acid sorption onto D-II07 resin. The sorption capacity of formic acid onto D-II07 resin was found to decrease slightly with the increase in solution temperature from 298 to 338 K, indicating the exothermic nature of the sorption reaction. This phenomenon agreed with the sorption equilibrium results (Fig. 4(A)–(C)) and the sorption thermodynamic analysis discussed above. The equilibrium time decreased from 60 to 35 min with increasing temperature from 298 to 338 K. These results probably attributed to the increase in diffusion rate of formic acid with increasing solution temperature. In addition, the formic acid sorption was fast at the initial stages of the contact period at various solution temperatures, and thereafter it became slower near the equilibrium. This was because of plenty of sorption sites that were available for sorption during the initial stage, and after a lapse of time, the remaining vacant surface sites were difficult to be occupied due to repulsive forces between the solute molecules on the solid and bulk phases [31]. Similar trend was observed in the sorp-

Table 3
Thermodynamic parameters for the sorption of formic acid onto D-II07 resin at different temperatures

T (K)	K_0	ΔG° (kJ mol^{-1})	ΔH° (kJ mol^{-1})	ΔS° (J mol^{-1} K^{-1})
298	1.103	−0.244		
318	1.091	−0.186	−1.165	−3.088
338	1.813	−0.093		

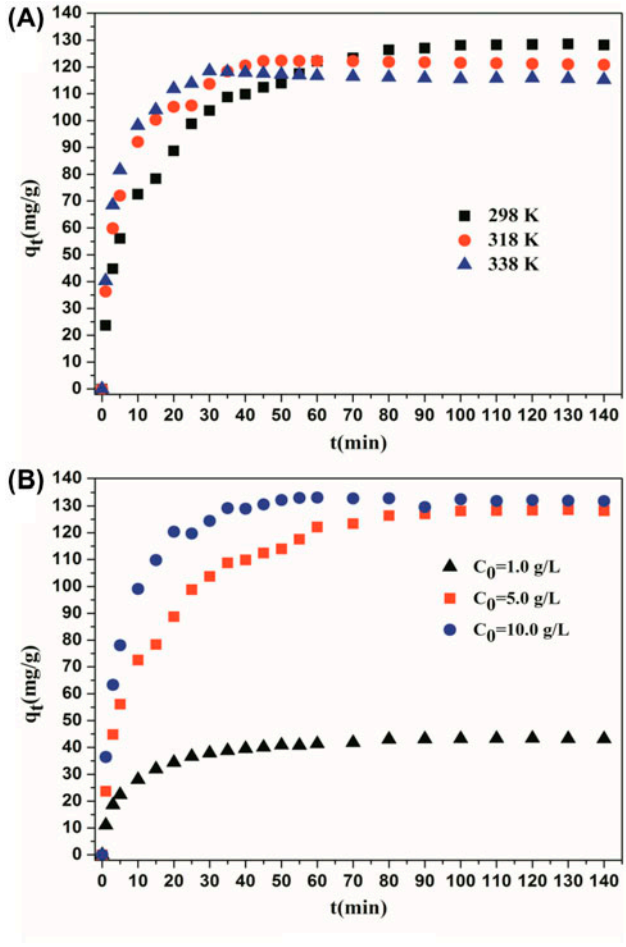

Fig. 6. The effect of contact time on the sorption of formic acid onto D-II07 resin at various temperatures (A); different initial concentrations of formic acid (B).

tion of formic acid on weakly basic adsorbent Amberlite IRA-67 [7].

3.6.2. Effect of initial concentration on formic acid sorption

The effect of initial concentration on the sorption time and sorption rate of formic acid onto D-II07 resin was investigated by changing the initial formic acid concentration in the range of 1–10 g L^{-1} at 298 K. Fig. 6(B) shows the effect of initial concentration on the formic acid uptake onto D-II07 resin. As it depicts, the sorption capacity of formic acid at equilibrium increase from 43 to 132 mg g^{-1}. This phenomenon may be explained by the saturation of accessible–exchangeable sites of adsorbents. The equilibrium time decreased from 90 to 45 min when increasing formic acid initial concentration from 1 to 10 g L^{-1} at 298 K. This was due to the fact that the mass transfer driving force increased with increasing initial concentration, resulting in rapid equilibrium.

3.6.3. Kinetic simulation analyses

Sorption kinetic describes the solute sorption rate and plays an important role in evaluating the efficiency of the sorption. Therefore, it is essential to be able to predict the rate at which formic acid is removed from aqueous solutions in order to design a sorption treatment plant. In order to clarify the sorption kinetics of formic acid onto D-II07 resin at various operating conditions, kinetic analyses were conducted using the macropore diffusion model, pseudo-first- and pseudo-second-order models.

The pseudo-first-order kinetic model equation can be written as follows [41]:

$$\frac{dq_t}{dt} = k_1(q_e - q_t) \tag{16}$$

where q_e and q_t are the amounts of formic acid adsorbed (mg g^{-1}) on the resin at equilibrium and at time t (min), respectively; k_1 is the pseudo-first-order rate constant for the sorption (min^{-1}).

Integrating Eq. (16) for the boundary conditions $t = 0$ to $t = t$ and $q_t = 0$ to $q_t = q_t$ gives:

$$\ln(q_e - q_t) = \ln q_e - k_1 t \tag{17}$$

Further modification gives:

$$C_t = (C_0 - C_e)e^{-k_1 t} + C_e \tag{18}$$

The pseudo-second-order kinetic model equation is generally given as follows [42]:

$$\frac{dq_t}{dt} = k_2(q_e - q_t)^2 \tag{19}$$

where q_e and q_t are the amounts of formic acid adsorbed (mg g^{-1}) on the resin at equilibrium and at time t (min), respectively; k_2 is the pseudo-second-order rate constant of sorption (min^{-1}).

Integrating Eq. (19) for the boundary conditions $t = 0$ to $t = t$ and $q_t = 0$ to $q_t = q_t$ gives:

$$\frac{1}{q_e - q_t} - \frac{1}{q_e} = k_2 t \tag{20}$$

Eq. (20) can be simplified as:

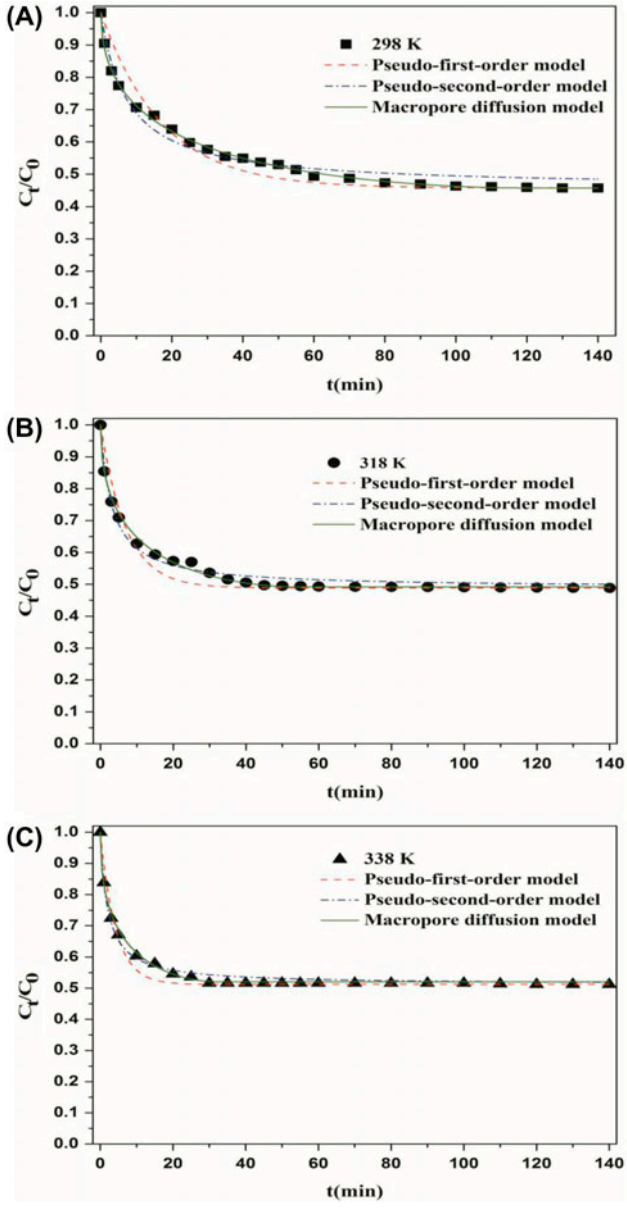

Fig. 7. Comparison of the macropore diffusion model, pseudo-first-order, and pseudo-second-order kinetic models for batch sorption of formic acid by D-II07 resin at different temperatures: (A) T = 298 K; (B) T = 318 K; and (C) T = 338 K.

$$q_t = \frac{k_2 q_e^2 t}{1 + k_2 q_e t} \tag{21}$$

Expressing the Eq. (21) in terms of C_t and C_e, the final equation is:

$$C_t = C_0 - \left(\frac{m}{V}\right) \frac{k_2[(V/m)(C_0 - C_e)]^2 t}{1 + k_2[(V/m)(C_0 - C_e)]t} \tag{22}$$

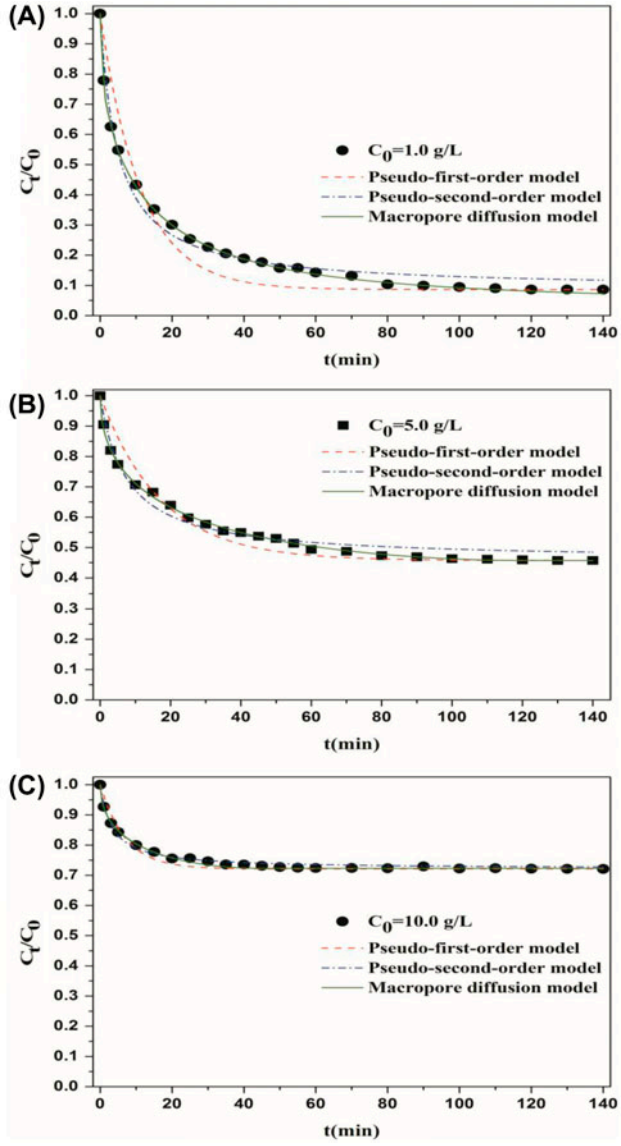

Fig. 8. Comparison of the macropore diffusion model, pseudo-first-order, and pseudo-second-order kinetic models for batch sorption of formic acid by D-II07 resin at different initial formic acid concentrations: (A) C_0 = 1 g L^{-1}; (B) C_0 = 5 g L^{-1}; and (C) C_0 = 10 g L^{-1}.

The average relative deviation(ARD%) used to evaluate the model fitness was calculated using the following equation:

$$\text{ARD}\% = \frac{1}{N}\sum_{i=1}^{N} \left| \frac{C_{exp} - C_{pred}}{C_{exp}} \right| \times 100 \tag{23}$$

where N is the number of experimental data point; C_{exp} is the experimental concentration of formic acid in solution (g L^{-1}); C_{pred} is the concentration of formic acid in the solution predicted with models (g L^{-1}).

The macropore diffusion model was adopted to give a comprehensive simulation to the sorption process, which considers the diffusion in the resin particle as a rate-limiting mechanism [43]. In the macropore diffusion model, the assumptions that were made to interpret the ion-exchange sorption are as follows: (i) the resin particle has a structure containing macropores; (ii) the resin with homogeneous size has a spherical geometry; (iii) external mass transfer is neglected due to efficient mixing; (iv) constant temperature operation; (v) equilibrium between the liquid phase in the macropores and the active site was instantaneous; and (vi) internal diffusion in the resin particle is rate-controlling.

Mass balance in the volume element of the resin particle is given as:

$$\varepsilon_p \frac{\partial C_p}{\partial t} + \rho_p \frac{\partial q}{\partial t} = D_p \left(\frac{\partial^2 C_p}{\partial R^2} + \frac{2}{R} \frac{C_p}{\partial R} \right) \quad (24)$$

The overall adsorber mass balance:

$$\frac{dC}{dt} = \left(\frac{1-\varepsilon}{\varepsilon} \right) \frac{3}{R_p} D_p \frac{\partial C_p}{\partial R}|_{R=R_P} \quad (25)$$

where ε is the external (batch) porosity.

$$\varepsilon = \frac{V_1}{V_1 + V_P} \quad (26)$$

The initial and boundary conditions are:

$$C(0) = C_0; t = 0 \quad (27)$$

$$C_p(R,0) = 0; 0 \leqslant R \leqslant R_p; t = 0 \quad (28)$$

$$\frac{\partial C_p}{\partial R}(0,t) = 0; t > 0 \quad (29)$$

$$C_p(R_p,t) = C(t); t > 0 \quad (30)$$

where C_p is the fluid-phase concentration in the macropores (g L^{-1}); C is the bulk fluid-phase concentration (g L^{-1}); q is the adsorbed phase concentration (g g^{-1}); ρ_p is the resin particle density (g L^{-1}); t is the time (s); R is the radial distance from the center of the resin pallet (m); R_p is the radius of the pellet (m); ε_p is the particle porosity; D_p is the effective pore diffusion coefficient (m^2 s^{-1}); V_1 is the liquid phase volume (L); V_P is the pellet volume (L).

In this sorption process, the concentration equilibrium between liquid and solid phase could be represented by the Sips isotherm model, which had a best fitting result with the experimental data. The, ARD% defined as Eq. (23), was used to evaluate the model fitness to the experimental data. The partial differential equations involved in the macropore diffusion model were solved numerically using PDESOL software. The value of D_p was obtained by the best fitting of the simulation results to the experimental data [18].

Figs. 7(A)–(C) and 8(A)–(C) show the fits of the macropore diffusion model, pseudo-first- and pseudo-second-order kinetic models to the experimental data at various operational conditions. The values of D_p, k_1, and k_2 for each model are listed in Table 4. It was concluded from the concentration decay curves at different temperatures that the concentration of the formic acid solution decreased gradually with time. According to the ARD% (Table 4), the fits of the pseudo-first- and pseudo-second-order models to the experimental data were not as good as the macropore diffusion model, indicating that the macropore diffusion model was applicable to describe the adsorption process of formic acid onto D-II07 resin. By least square fitting, the effective pore diffusion coefficients at 298, 318, and 338 K were 1.846×10^{-10}, 3.652×10^{-10}, and 5.552×10^{-10} m^2 s^{-1}, respectively (Table 4). The

Table 4
Coefficients of the macropore diffusion model, pseudo-first-, and pseudo-first-second-order models at different temperatures and initial formic acid concentrations

		Macropore diffusion model				Pseudo-first-order model		Pseudo-second-order model	
T (K)	C_0 (g L^{-1})	D_p ($\times 10^{-10}$ m^2 s^{-1})	D_m ($\times 10^{-9}$ m^2 s^{-1})	D_p/D_m	ARD%	k_1 (min^{-1})	ARD%	k_2 (min^{-1})	ARD%
298	**5.0**	1.846	1.695	0.109	0.769	0.0579	4.112	0.991	3.703
318	5.0	3.652	2.752	0.133	0.840	0.143	3.334	2.439	2.915
338	5.0	5.552	3.989	0.139	1.126	0.236	2.073	4.006	2.096
298	**1.0**	1.804	1.695	0.106	3.482	0.0890	20.025	4.437	15.319
298	**10.0**	1.825	1.695	0.108	0.528	0.143	1.383	2.192	0.937

Note: The bold values were used to distinguish two different operating conditions, such as temperature and initial formic acid concentration.

effective pore diffusivity (D_p) increased by 1.5–2-fold as the temperature increased by 20˚C each in the range of 298–338 K. Although the same trends (1.5–2.5-fold) can be obtained from the pseudo-first- and pseudo-second models rate constants, the ARD% for pseudo-first- and pseudo-second-order models were comparatively large. It could be further illustrated in Fig. 9(A)–(C), which described the trend in concentration change vs. different radials at various times for 298, 318, and 338 K simulated with the macropore diffusion model. In Fig. 9(A)–(C), the concentration gradients of 338 K at each time were always larger than those of 298 K before they all absolutely reached the equilibrium. Another conclusion could be drawn from Table 4 that the values of D_p were stable when the initial concentration varied at constant temperature, which indicated that the effective pore diffusivity was independent of concentration. Consequently, these results indicated that with the increase in temperature, the effective pore diffusivity became larger (Table 4), and the time to reach equilibrium was shorter.

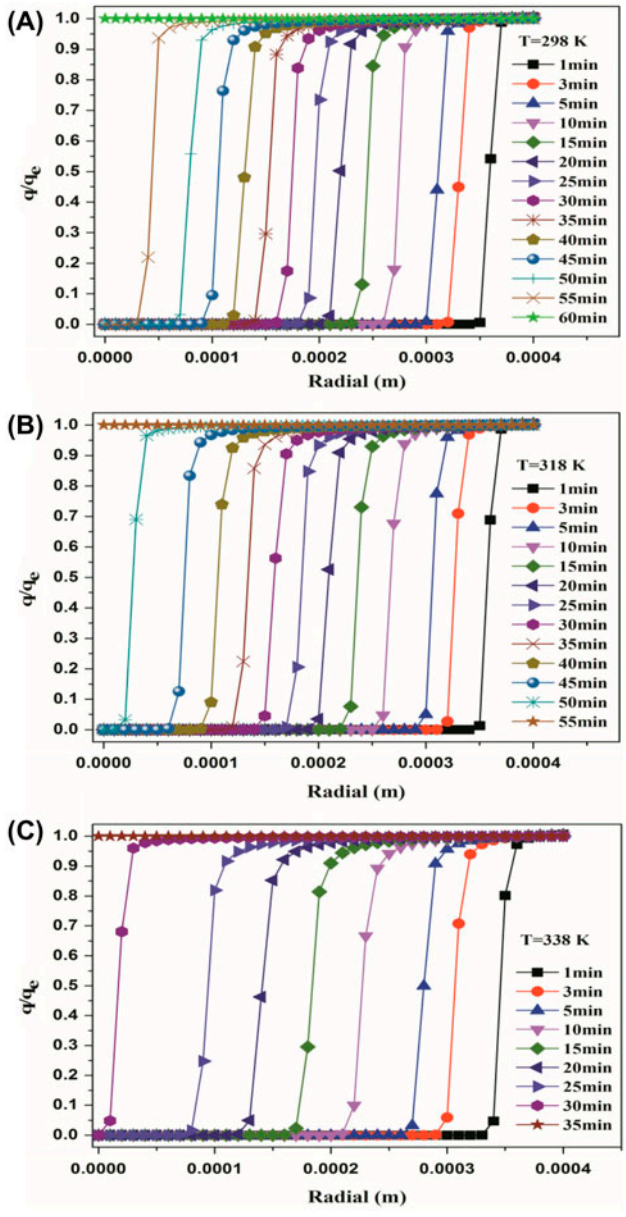

Fig. 9. Evolution of the dimensionless radial formic acid concentration profiles, q/q_e vs. R inside the D-II07 resin particle calculated from the macropore diffusion model for batch adsorption at different temperatures; $C_0 = 5$ g L^{-1}. (A) $T = 298$ K; (B) $T = 318$ K; and (C) $T = 338$ K.

For comparing with the diffusion of formic acid in the resin particle, the molecular diffusivity of formic acid was calculated by the Wilke and Chang correlation [44]:

$$D_m = 7.4 \times 10^{-8} \frac{(\alpha_A M_s)^{0.5} T}{\mu V_m^{0.6}} \quad (31)$$

where α_A is a constant which accounts for solute–solvent interactions, and the value is 2.6 for water; μ is the viscosity of water at different temperature (cP); M_s is the molecular weight of the solvent (g mol^{-1}); V_m is the molar volume of the liquid solute at its normal boiling point (mL g^{-1} mol^{-1}); T is the temperature (K). The diffusion coefficient of formic acid in water (D_m) and the ratio of D_p/D_m were all calculated and listed in Table 4. The diffusion rate in the resin particle (D_p) was slower than that in the solution (D_m), which indicated that the intraparticle diffusion was the rate-limiting step in the adsorption process of formic acid onto D-II07 resin.

4. Conclusions

In the present investigation, D-II07 resin exhibited good potentials for further research and practical applications in the efficient removal of formic acid from the diluted fermentation broth or wastewater. The bi-Langmuir isotherm model described the experimental data best over the entire concentration range studies. Based on the thermodynamic results, the sorption was a spontaneous and exothermic process. The macropore diffusion model was more suitable for predicting the sorption process. The effective pore diffusivity (D_p) was dependent on temperature, but independent of initial formic acid concentration. The D_p at 298, 318, and 338 K was 1.846×10^{-10}, 3.652×10^{-10}, and 5.552×10^{-10} m^2 s^{-1}, respectively.

Acknowledgments

The authors acknowledge the financial support of Plan Project of National Science and Technology (2012BAD32B07), the Industrialization Project of High-new Technology of Guangdong Province (2013B010404036, 2013B010403020), the project of National Natural Science Foundation of China (51378486, U1261116), Natural Science Foundation of Guangdong Province (S2012040007546), Guangzhou Science and Technology (2013J4300031), the Project of Jiangsu Province Science and Technology (BE2013083), the Foundation of Xuyi Center of Attapulgite Applied Technology Research Development & Industrialization, Chinese Academy of Sciences (20121004), and the Foundation of Director of Guangzhou Institute of Energy Conversion, Chinese Academy of Sciences (y407r41001).

References

[1] D. Datta, S. Kumar, Intensification of recovery of formic acid from aqueous stream using reactive extraction with N, N-dioctyloctan-1-amine: Effect of diluent and temperature, Chem. Eng. Commun. 200 (2013) 678–700.
[2] H.-G. Nam, G.-W. Lim, S. Mun, Separation of acetic acid, formic acid, succinic acid, and lactic acid using adsorbent resin, J. Chem. Eng. Data 57 (2012) 2102–2108.
[3] V.M. Bhandari, V.A. Juvekar, S.R. Patwardhan, Sorption studies on ion exchange resins. 2. Sorption of weak acids on weak base resins, Ind. Eng. Chem. Res. 31 (1992) 1073–1080.
[4] C. Huang, X.-X. Cui, H. Wu, W.-Y. Lou, M.-H. Zong, The effect of different factors on microbial oil production by *Trichosporon fermentans* on rice straw acid hydrolysate, Int. J. Green Energ. 11 (2014) 787–795.
[5] E. Palmqvist, B. Hahn-Hägerdal, Fermentation of lignocellulosic hydrolysates. II: Inhibitors and mechanisms of inhibition, Bioresour. Technol. 74 (2000) 25–33.
[6] H. Uslu, I.S. İnci, S.A.S. Bayazit, Adsorption equilibrium data for acetic acid and glycolic acid onto Amberlite IRA-67, J. Chem. Eng. Data 55 (2010) 1295–1299.
[7] H. Uslu, Adsorption equilibria of formic acid by weakly basic adsorbent Amberlite IRA-67: Equilibrium, kinetics, thermodynamic, Chem. Eng. J. 155 (2009) 320–325.
[8] Z. Wu, S.T. Yang, Extractive fermentation for butyric acid production from glucose by *Clostridium tyrobutyricum*, Biotechnol. Bioeng. 82 (2003) 93–102.
[9] G. Luo, S. Pan, J. Liu, Use of the electrodialysis process to concentrate a formic acid solution, Desalination 150 (2002) 227–234.
[10] B.-J. Liu, Q.-L. Ren, Sorption of levulinic acid onto weakly basic anion exchangers: Equilibrium and kinetic studies, J. Colloid Interface Sci. 294 (2006) 281–287.
[11] W.-Y. Tong, X.-Y. Fu, S.-M. Lee, J. Yu, J.-W. Liu, D.-Z. Wei, Y.-M. Koo, Purification of $_L$(+)-lactic acid from fermentation broth with paper sludge as a cellulosic feedstock using weak anion exchanger Amberlite IRA-92, Biochem. Eng. J. 18 (2004) 89–96.
[12] W. Takatsuji, H. Yoshida, Removal of organic acids from wine by adsorption on weakly basic ion exchangers: Equilibria for single and binary systems, Sep. Sci. Technol. 29 (1994) 1473–1490.
[13] N. Kanazawa, K. Urano, N. Kokado, Y. Urushigawa, Adsorption equilibrium equation of carboxylic acids on anion-exchange resins in water, J. Colloid Interface Sci. 238 (2001) 196–202.
[14] N. Kanazawa, K. Urano, N. Kokado, Y. Urushigawa, Exchange characteristics of monocarboxylic acids and monosulfonic acids onto anion-exchange resins, J. Colloid Interface Sci. 271 (2004) 20–27.
[15] V.M. Bhandari, T. Yonemoto, V.A. Juvekar, Investigating the differences in acid separation behaviour on weak base ion exchange resins, Chem. Eng. Sci. 55 (2000) 6197–6208.
[16] H. Yoshida, W. Takatsuji, Parallel transport of an organic acid by solid-phase and macropore diffusion in a weakly basic ion exchanger, Ind. Eng. Chem. Res. 39 (2000) 1074–1079.
[17] W. Qian, X. Lin, X. Zhou, X. Chen, J. Xiong, J. Bai, H. Ying, Studies of equilibrium, kinetics simulation and thermodynamics of cAMP adsorption onto an anion-exchange resin, Chem. Eng. J. 165 (2010) 907–915.
[18] X. Lin, J. Wu, J. Fan, W. Qian, X. Zhou, C. Qian, X. Jin, L. Wang, J. Bai, H. Ying, Adsorption of butanol from aqueous solution onto a new type of macroporous adsorption resin: Studies of adsorption isotherms and kinetics simulation, J. Chem. Technol. Biotechnol. 87 (2012) 924–931.
[19] S. Li, H. Guo, C. Luo, H. Zhang, L. Xiong, X. Chen, L. Ma, Effect of iron promoter on structure and performance of K/Cu–Zn catalyst for higher alcohols synthesis from CO_2 hydrogenation, Catal. Lett. 143 (2013) 345–355.
[20] G. Kortüm, K. Andrussow, Dissociation Constants of Organic Acids in Aqueous Solution, Butterworths, London, 1961.
[21] S. Larsson, E. Palmqvist, B. Hahn-Hägerdal, C. Tengborg, K. Stenberg, G. Zacchi, N.-O. Nilvebrant, The generation of fermentation inhibitors during dilute acid hydrolysis of softwood, Enzyme Microb. Technol. 24 (1999) 151–159.
[22] T. Shi, Z. Wang, Y. Liu, S. Jia, D. Changming, Removal of hexavalent chromium from aqueous solutions by D301, D314 and D354 anion-exchange resins, J. Hazard. Mater. 161 (2009) 900–906.
[23] X.-P. Liao, B. Shi, Adsorption of fluoride on zirconium (IV)-impregnated collagen fiber, Environ. Sci. Technol. 39 (2005) 4628–4632.
[24] S. Yadav, V. Srivastava, S. Banerjee, C.-H. Weng, Y.C. Sharma, Adsorption characteristics of modified sand for the removal of hexavalent chromium ions from aqueous solutions: Kinetic, thermodynamic and equilibrium studies, Catena 100 (2013) 120–127.
[25] F. Gode, E. Pehlivan, Removal of chromium(III) from aqueous solutions using Lewatit S 100: The effect of pH, time, metal concentration and temperature, J. Hazard. Mater. 136 (2006) 330–337.

[26] D.P. Das, J. Das, K. Parida, Physicochemical characterization and adsorption behavior of calcined Zn/Al hydrotalcite-like compound (HTlc) towards removal of fluoride from aqueous solution, J. Colloid Interface Sci. 261 (2003) 213–220.
[27] W. Stumm, Aquatic Surface Chemistry: Chemical Processes at the Particle-water Interface, Wiley, New York, NY, 1987.
[28] I. Langmuir, The constitution and fundamental properties of solids and liquids. Part I. Solids, J. Am. Chem. Soc. 38 (1916) 2221–2295.
[29] T.W. Webi, R.K. Chakravort, Pore and solid diffusion models for fixed-bed adsorbers, AIChE J. 20 (1974) 228–238.
[30] H. Freundlich, Über die adsorption in lösungen (Over the adsorption in solution), Z. Phys. Chem. 57 (1906) 385–470.
[31] I. Tan, A. Ahmad, B. Hameed, Adsorption isotherms, kinetics, thermodynamics and desorption studies of 2, 4, 6-trichlorophenol on oil palm empty fruit bunch-based activated carbon, J. Hazard. Mater. 164 (2009) 473–482.
[32] F. Haghseresht, G. Lu, Adsorption characteristics of phenolic compounds onto coal-reject-derived adsorbents, Energ. Fuels 12 (1998) 1100–1107.
[33] R. Sips, On the structure of a catalyst surface, J. Chem. Phys. 16 (1948) 490–495.
[34] K.K. Choy, G. McKay, J.F. Porter, Sorption of acid dyes from effluents using activated carbon, Resour. Conserv. Recycl. 27 (1999) 57–71.
[35] E. Repo, T.A. Kurniawan, J.K. Warchol, M.E. Sillanpää, Removal of Co(II) and Ni(II) ions from contaminated water using silica gel functionalized with EDTA and/or DTPA as chelating agents, J. Hazard. Mater. 171 (2009) 1071–1080.
[36] J. Huang, K. Huang, S. Liu, Q. Luo, S. Shi, Synthesis, characterization, and adsorption behavior of aniline modified polystyrene resin for phenol in hexane and in aqueous solution, J. Colloid Interface Sci. 317 (2008) 434–441.
[37] X. Zhou, J. Fan, N. Li, W. Qian, X. Lin, J. Wu, J. Xiong, J. Bai, H. Ying, Adsorption thermodynamics and kinetics of uridine 5′-monophosphate on a gel-type anion exchange resin, Ind. Eng. Chem. Res. 50 (2011) 9270–9279.
[38] A.A. Khan, R. Singh, Adsorption thermodynamics of carbofuran on Sn (IV) arsenosilicate in H^+, Na^+ and Ca^{2+} forms, Colloid Surf. 24 (1987) 33–42.
[39] I. Tan, A.L. Ahmad, B. Hameed, Adsorption of basic dye on high-surface-area activated carbon prepared from coconut husk: Equilibrium, kinetic and thermodynamic studies, J. Hazard. Mater. 154 (2008) 337–346.
[40] V. Gupta, P. Singh, N. Rahman, Adsorption behavior of Hg(II), Pb(II), and Cd(II) from aqueous solution on Duolite C-433: a synthetic resin, J. Colloid Interface Sci. 275 (2004) 398–402.
[41] S. Lagergren, Zur Theorie der sogenannten Absorption gelöster Stoffe (About the theory of so-called adsorption of soluble substances), K. Sven. Vetensk-apsakad, Handl. 24 (1898) 1–39.
[42] Y.-S. Ho, G. McKay, Kinetic models for the sorption of dye from aqueous solution by wood, Process Saf. Environ. Prot. 76 (1998) 183–191.
[43] M. Minceva, A. Rodrigues, Adsorption of xylenes on faujasite-type zeolite: Equilibrium and kinetics in batch adsorber, Chem. Eng. Res. Des. 82 (2004) 667–681.
[44] C. Wilke, P. Chang, Correlation of diffusion coefficients in dilute solutions, AIChE J. 1 (1955) 264–270.